Monthly Notices
of the
ROYAL ASTRONOMICAL SOCIETY

MNRAS **466,** 4272–4278 (2017)
Advance Access publication 2016 December 17

doi:10.1093/mnras/stw3277

Dark jets in the soft X-ray state of black hole binaries?

S. Drappeau,[1,2]★ J. Malzac,[1,2]★ M. Coriat,[1,2] J. Rodriguez,[3] T. M. Belloni,[4] R. Belmont,[1,2,3] M. Clavel,[3,5] S. Chakravorty,[6,7,8] S. Corbel,[3] J. Ferreira,[6,7] P. Gandhi,[9] G. Henri[6,7] and P.-O. Petrucci[6,7]

[1]*Université de Toulouse, UPS-OMP, IRAP, Toulouse, France*
[2]*CNRS, IRAP, 9 Av. colonel Roche, BP 44346, F-31028 Toulouse cedex 4, France*
[3]*Laboratoire AIM (CEA/IRFU – CNRS/INSU – Université Paris Diderot), CEA DRF/IRFU/SAp, F-91191 Gif-sur-Yvette, France*
[4]*Osservatorio Astronomico di Brera, Istituto Nazionale di Astrofisica, Via E. Bianchi 46, I-23807 Merate, Italy*
[5]*Space Sciences Laboratory, University of California, Berkeley, CA 94720, USA*
[6]*Université Grenoble Alpes, IPAG, F-38000 Grenoble, France*
[7]*CNRS, IPAG, F-38000 Grenoble, France*
[8]*Department of Physics, Indian Institute of Science, Bangalore, 560012, India*
[9]*Department of Physics and Astronomy, University of Southampton, Highfield, Southampton SO17 1BJ, UK*

Accepted 2016 December 14. Received 2016 December 13; in original form 2016 April 14

ABSTRACT

X-ray binary observations led to the interpretation that powerful compact jets, produced in the hard state, are quenched when the source transitions to its soft state. The aim of this paper is to discuss the possibility that a powerful dark jet is still present in the soft state. Using the black hole X-ray binaries GX339–4 and H1743–322 as test cases, we feed observed X-ray power density spectra in the soft state of these two sources to an internal shock jet model. Remarkably, the predicted radio emission is consistent with current upper limits. Our results show that for these two sources, a compact dark jet could persist in the soft state with no major modification of its kinetic power compared to the hard state.

Key words: accretion, accretion discs – black hole physics – radiation mechanisms: non-thermal – relativistic processes – shock waves – X-rays: binaries.

1 INTRODUCTION

The properties of outflows launched by accreting black holes in X-ray binary systems appear to be deeply connected to the state of the accretion flow (see e.g. Done, Gierliński & Kubota 2007; Fender & Gallo 2014; Malzac 2016). In their hard X-ray spectral state, black hole X-ray binaries emit powerful compact jets. Those jets radiate partially self-absorbed synchrotron emission that is routinely detected in the radio band (Fender et al. 2000; Fender 2001) with flat or weakly inverted spectral slopes ($F_\nu \propto \nu^\alpha$ with $\alpha \simeq -0.5$ to 0). This emission can extend at higher frequencies up to the IR and optical bands (Corbel & Fender 2002; Chaty, Dubus & Raichoor 2011; Gandhi et al. 2011). In the prototypical source Cyg X-1, GeV emission was recently detected by *Fermi* (Malyshev, Zdziarski & Chernyakova 2013; Zanin et al. 2016) and interpreted as inverse Compton emission from the jet (Zdziarski et al. 2014, 2016). Also, in this source, the strong polarization fraction recently detected by *INTEGRAL* above 400 keV (Laurent et al. 2011; Jourdain et al. 2012; Rodriguez et al. 2015) suggests that the MeV tail observed in the hard state (McConnell et al. 2000; Jourdain, Roques & Malzac 2012; Zdziarski, Lubiński & Sikora 2012) originates from optically thin synchrotron emission in the jet.

In some cases, radio jet structures have been resolved at the astronomical units scale (Stirling et al. 2001; Fuchs et al. 2003). Observations suggest that the jet kinetic power in the hard state could be comparable to, or even larger than, the X-ray luminosity (Gallo, Fender & Pooley 2003; Gallo et al. 2005; Körding, Fender & Migliari 2006). In contrast, compact jets are not detected in the soft state. The current radio upper limits indicate that the emission is suppressed by several orders of magnitude at least (Corbel et al. 2000; Russell et al. 2011). This led to the generally accepted view that the jets are not produced in the soft state (Fender, Belloni & Gallo 2004; Fender, Homan & Belloni 2009).

Here we will argue that compact jets could still be present in the soft state, with a kinetic power comparable to that in the hard state, and that only their emission is quenched. This is an important issue also because this would affect the estimates of the global kinetic feedback of accreting black holes with consequences for the large-scale impact of supermassive black holes on their environment.

A popular model for the radio-IR emission of black hole jets is the internal shock model. (Rees 1978; Rees & Meszaros 1994; Daigne & Mochkovitch 1998; Kaiser, Sunyaev & Spruit 2000;

★ E-mail: drappeau.samia@gmail.com (SD); julien.malzac@irap.omp.eu (JM)

Spada et al. 2001; Böttcher & Dermer 2010; Jamil, Fender & Kaiser 2010; Malzac 2013). In this model, velocity fluctuations injected at the base of the jet drive internal shocks at large distances from the black hole. Leptons are accelerated at the shocks and emit synchrotron radiation. Malzac (2013, 2014) showed that the total radiated power and the spectral energy distribution (SED) are very sensitive to the amplitude and time-scales of the velocity fluctuations. The origin of the velocity fluctuations is not specified in the model but are likely to be driven by the fluctuations of the accretion flow that in turn can be traced by the X-ray light curve. If this is the case, the jet velocity fluctuations are expected to be similar to the observed X-ray fluctuations. Therefore, assuming the jet Lorentz factor variation have the same Fourier power density spectrum (PDS) as the observed X-ray PDS, the model should predict a radio-IR jet spectral energy distribution that is close to the observations. The results of Drappeau et al. (2015, hereafter D15) suggest that this is indeed the case. They used one of the most complete multiwavelength observation of GX339–4 in the hard state and successfully modelled the radio-IR SED using the observed X-ray PDS as input of the model.

The typical rms amplitude of the fast ($\lesssim$1 ks) X-ray variability is in the range 10–30 per cent in the hard state, and decreases to less than a few per cent in the soft state (see e.g. Belloni & Stella 2014). In the framework of the internal shock model, smaller amplitude fluctuations of the jet Lorentz factor imply weaker shocks and less energy available to particle acceleration and radiation. The resulting radio flux scales approximately like $\sigma^{2.8}$, where σ is the fractional rms amplitude of fluctuations (see Malzac 2013, equation 39). Therefore, if the amplitude of the jet fluctuations tracks the X-ray variability also in the soft state, the radio emission is expected to drop by several orders of magnitude with respect to the hard state level, even if the jet kinetic power remains unchanged.

In this paper, we investigate whether this effect could be sufficient to explain the observed disappearance of the radio emission in the soft state. We model the radio emission of two black hole binaries GX339–4 and H1743–322 in the soft state using the internal shock model ISHEM (Malzac 2014) and compare the results to the observational upper limits. The data and model are described in Sections 2 and 3, respectively. We find that the weak fluctuations observed in the soft state produce weak radio emission compatible with the current upper limits, whereas the total kinetic power of such dark jets can be as large as in the hard state. These findings are discussed in Sections 4 and 5.

2 OBSERVATIONS AND DATA REDUCTION

For both GX339–4 and H1743–322, we use X-ray PDS obtained from soft-state observations. In the case of H1743–322, we focused on a single observation that was obtained in (quasi-)simultaneity with a radio observation. The *Rossi X-ray Timing Explorer* (*RXTE*) observations were carried out on 2003 August 11. For GX339–4, since no simultaneous radio-X-ray observations were available, we accumulated all the data obtained during the soft state of the 2010 outburst (from 2010 May 14 to December 30; see e.g. Clavel et al. 2016). This allowed us to increase the statistical significance of the PDS obtained.

For both sources, we produced ∼4 ms (2^{-8} s) resolution light curves from the Proportional Counter Array (PCA) onboard *RXTE*. The data were reduced in a standard manner (e.g. Rodriguez & Varnière 2011; Clavel et al. 2016) with the HEASOFT V6.16 software suite. The light curves were obtained from event mode data between ∼2 and ∼50 keV (spectral channels 0–116) in order to limit the background noise above this energy. We also checked that no differences in the final result were obtained while limiting further the energy range to ∼2–20 keV. PDS from each individual observation were produced on intervals of 96 s, all intervals were further averaged and, in the case of GX339–4, all observations were combined to produce a single PDS. The dead time-corrected white noise was subtracted from the PDS. The resulting soft-state PDS of GX339–4 and H1743–322 are shown in Fig. 1, together with the hard-state PDS of GX339–4 used in D15. The 0.07–5 Hz fractional rms amplitudes are, respectively, 1.9, 2.3 and 27 per cent.

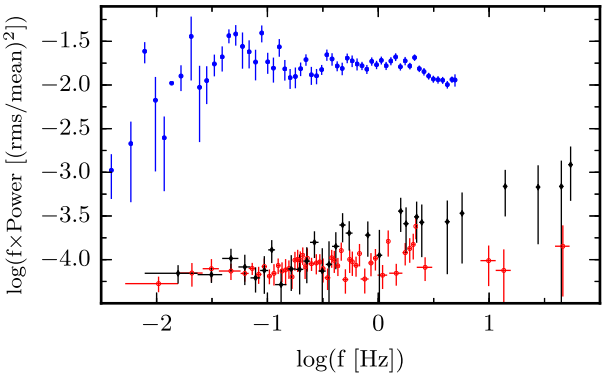

Figure 1. Soft-state X-ray PDS of GX339–4 (red circle) and H1743–322 (black diamond) in the 2–50 keV band, used to constrain the fluctuations of the bulk Lorentz factor of the ejecta. For comparison, the X-ray PDS of GX339–4 in the hard state is also shown (blue filled circle).

Radio observations of GX339–4 used in this study were conducted with the Australia Telescope Compact Array on 2010 June 25 and 2010 August 22 when GX339–4 was in the soft state. The array was in the extended 6C and compact H168 configurations during the June and August observations, respectively. We observe the source at 5.5 and 9 GHz simultaneously. Each frequency band was composed of 2048 1-MHz channels. For both observations, we used PKS B1934-638 for absolute flux and calibration and PKS J1646-50 to calibrate the antenna gains as a function of time. Flagging, calibration and imaging were carried out with the Multichannel Image Reconstruction, Image Analysis and Display software (MIRIAD; Sault, Teuben & Wright 1995). We did not detect the source in any of the observations. To obtain the best constraint on jet emission of GX339–4, we combined the two observations at imaging step and obtain a 3σ upper limit of 24 μJy. The optical and near-infrared (hereafter OIR) observations were taken with the ANDICAM camera on the SMARTS 1.3 m telescope located at Cerro Tololo in Chile (see Buxton et al. 2012). The values used for this study are an average of the different measurements taken between the two radio observations. The error is estimated from the variance of the flux over that period.

The radio 8.46 GHz upper limit of 30 μJy used for the study of H1743–322 have been published by McClintock et al. (2009) based on a Very Large Array observation conducted on MJD 52863 during the soft state of its 2003 outburst. The OIR observations have been published by Chaty, Muñoz Arjonilla & Dubus (2015). We refer the reader to these articles for further details.

3 JET EMISSION MODEL

3.1 ISHEM model

We use the numerical code ISHEM that simulates the hierarchical merging and the emission of ejecta constituting a jet. At each time

step Δt, a new shell of matter is ejected. Δt is comparable to the dynamical time-scale at the initial ejecta radius $r_{\rm dyn}$. Each new created shell has a specific Lorentz factor γ. Its value depends on the time of the ejection, so that the overall distribution of its fluctuations follows the shape of a given PDS. All shells, the one injected and the one resulting from mergers, are tracked throughout the duration of the simulation until they merge with other shells. When propagating outwards, adiabatic losses cause the shells to gradually lose their internal energy. Eventually, while merging, part of their bulk kinetic energy is converted into internal energy and radiation. The details of the physics and the description of the main parameters of the model are presented in the original paper (Malzac 2014).

3.2 Input parameters from GX339–4 and H1743–322

The low-mass black hole binary GX339–4 is a recurrent X-ray transient. The source properties are not well-constrained. Here we assume a black hole mass of 10 $M_\odot$, a distance of 8 kpc and an inclination angle of 23° compared to the line of sight. These parameters are within the observational uncertainties (Zdziarski et al. 2004; Shidatsu et al. 2011) and identical to those used in D15. H1743–322 is an X-ray binary and a black hole candidate, exhibiting recurrent outbursts. We assume a mass of 10 $M_\odot$, an inclination angle of 75° and a distance of 8.5 kpc (Steiner, McClintock & Reid 2012). For both sources, the jet half-opening angle ϕ is set to 1° (unless otherwise stated) and the time-averaged jet Lorentz factor is set to $\langle\Gamma\rangle = 2$ in agreement with current observational constraints (Fender et al. 2009).

An important parameter of the model is the kinetic power available to the jet. In the case of GX339–4, we choose the value estimated in D15 to be able to perform comparison with the study done in the hard state for this source, $P_{\rm jet} \simeq 0.05\,L_{\rm Edd}$. As for H1743–322, the total power of the jets is set to equal the observed X-ray luminosity, i.e. $P_{\rm jet} = 0.06\,L_{\rm Edd}$. Note that $P_{\rm jet}$ is the total kinetic power of the two-sided jets. Only a fraction (potentially very small) of this total kinetic power can be radiated away.[1]

Besides these inputs, the time-distribution of the fluctuations of the kinetic energy ($\gamma - 1$) has a power spectrum that follows the shape (and amplitude) of the observed X-ray PDS, for both sources, in the soft state (see Fig. 1). We extrapolate the shape at low frequencies (down to 10^{-5} Hz) and high frequencies (up to 50 Hz), assuming in both case $PDS \propto \frac{1}{f}$.

3.3 Simulation and outputs

To produce the emission of fully developed jet and counter-jet, we run our simulations for a time $t_{\rm simu} = 10^5$ s (∼1 d), as measured in the observer's frame. Self-absorbed synchrotron from a non-thermal population of electrons is the only radiation process considered here. The electrons have a power-law distribution with a spectral index of $p = 2.3$, between minimum energy $\gamma_{\rm min} = 1$ and maximum energy $\gamma_{\rm max} = 5 \times 10^3$. These values are set and fixed throughout the simulation. The choice of $p = 2.3$ is consistent with the typical value expected in shock acceleration. These parameters are identical to those used in D15 except for $\gamma_{\rm max}$ that was reduced (from 10^6 to 5×10^3) to suppress any contribution of the jet emission in the *RXTE* band (see the discussion in Section 4).

The emission from each individual shell created during the simulation is time-averaged over the simulation running time $t_{\rm simu}$ to produce the final SED. The general shape of the simulated SED is determined solely by the shape of the PDS we used. The other free parameters of the model only allow us to modify the flux normalization or to shift it with respect to the photon frequency. The broad-band spectra are computed from 10^7 to 10^{16} Hz.

To assess the plausibility of our model, we compare the simulated SEDs to the radio upper limits obtained from the observations (see Section 2).

4 RESULTS

Fig. 2 (left) compares a simulated SED to the observed SED of GX339–4 in the soft state. The simulated and observed SEDs in the hard state of D15 are also shown for comparison on the right. The soft-state dash–dotted SED shows the result of a simulation in which all our model parameters for the soft state are identical to those of the hard state, except for the shape of the fluctuations of the jet bulk Lorentz factor. The significant difference between the hard- and soft state-simulated SEDs is then only due to the different PDS. We see that compared to the hard state, the predicted radio flux (shown in dash-dot lines) drops by almost three orders of magnitude in the soft state. However, it is right above the observational upper limits and therefore should have been detected. Nevertheless, slightly widening the jet half-opening angle to 3° drops the radio flux by half an order of magnitude, below the observational upper limit. This simulation is shown by the thick black curve on the left-hand panel of Fig. 2. The predicted radio fluxes for a 2.5 and a 3.5 half-opening angle are also shown. For larger opening angles, the same amount of dissipation occurs in a larger jet volume. As a result, the particle's energy density and magnetic field are reduced, which in turn reduces the synchrotron emission.

Fig. 3 shows the simulated SED of H1743–322, compared to radio upper limits and infrared observational data in the soft state. The predicted SED in the soft state is consistent with the observational constraints. In both figures, the optical/infrared (OIR) emission in the soft state is assumed to originate from the outer parts of the accretion disc (Coriat et al. 2009), therefore we do not attempt to fit the OIR data with our jet model.

A detailed modelling of the accretion flow is out of the scope of this work, however, for illustration purpose, we fitted the OIR to X-ray data shown in Figs 2 and 3 with the self-irradiated accretion flow model DISKIR (Gierliński, Done & Page 2008, 2009), combined with a Gaussian to model the Fe K_α line and reflection when needed. The results are shown by the dashed lines in Figs 2 and 3. The parameters of the DISKIR models are listed in Table 1. Although these parameters were obtained using a proper fit procedure leading to a good statistical representation of the data (reduced χ^2 close to unity), these are probably not the best fits. In fact, we found considerable model degeneracy and that most of the model parameters are poorly constrained. We did not attempt to explore the parameter space or make quantitative calculations of the parameter uncertainties. These models are just shown as example of plausible accretion flow parameters that give a reasonable description of the data.

Regarding the hard-state model, we note that the maximum energy of the radiating electrons used in D15 ($\gamma_{\rm max} = 10^6$) implies that the jet produces synchrotron radiation up to tens of MeVs.

[1] In the case of blazar jets, this radiated fraction may reach 10 per cent of their kinetic power (Ghisellini et al. 2014), which is achievable in the colliding shell model if the amplitude of the velocity fluctuations is large enough. In the framework of gamma-ray bursts, Beloborodov (2000) finds that the radiative efficiency of internal shocks can reach almost 100 per cent.

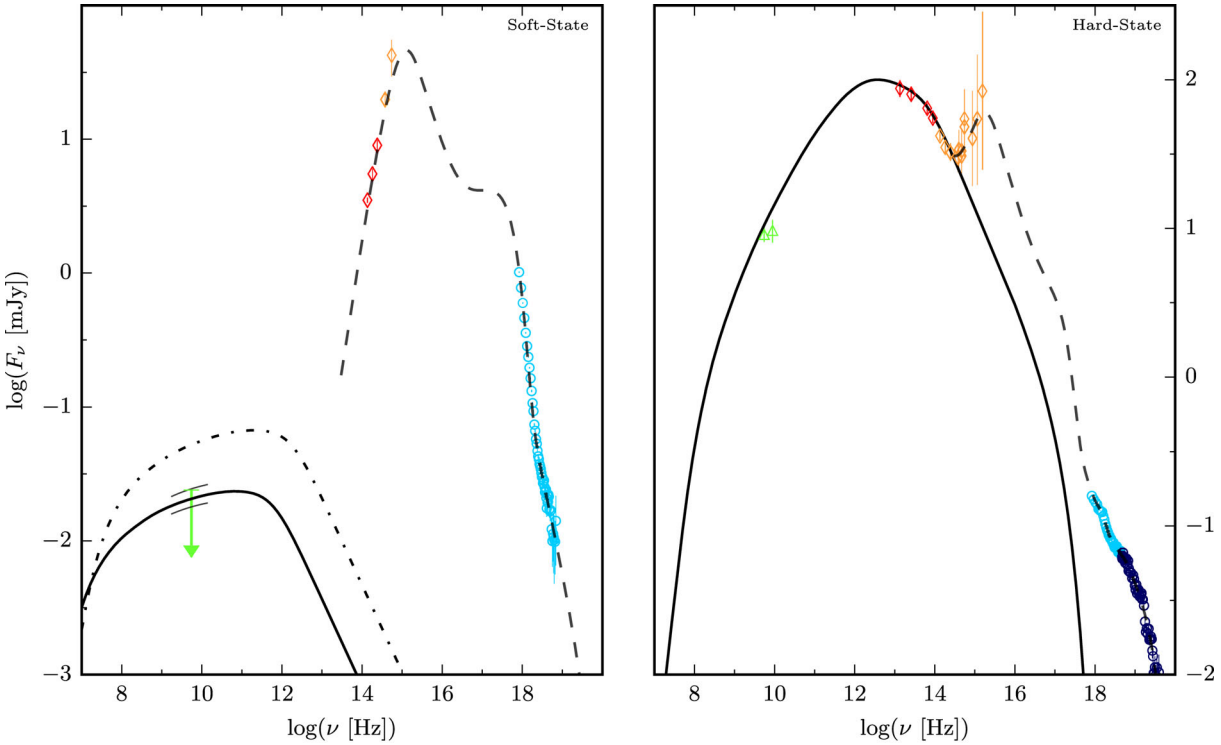

Figure 2. Broadband spectra of GX339–4 in the soft state (left) compared to that of the hard state (right), studied in D15. Colour code of the observed data is as follows: in green are the radio observations and upper limits, in red are the infrared bands, in orange the optical and ultraviolet and in blue the X-ray (light blue is PCA, dark blue is HEXTE. Soft-state PCA data were observed on 2010 May 19). The vertical error bars represent the statistical and systematic errors on the mean. On the left-hand panel, the total self-absorbed synchrotron jet emission from our two models ($\phi = 3^\circ$ and 1°) are shown as solid and dot–dashed black lines, respectively. The two thin black curves around the radio upper limit represent the radio flux predicted from a $2\overset{\circ}{.}5$ and a $3\overset{\circ}{.}5$ half-opened jet. The spectra have been averaged over the whole duration of the simulation. The OIR to X-ray emission is assumed to originate from the accretion flow and the data are fit with the irradiated accretion disc DISKIR model, shown in dashed lines in both panels. We note that the right-hand panel corrects fig. 2 of D15 in which the *RXTE* data were erroneously plotted with a normalization that was too large by a factor of 1.5. Also differently than the model SED of D15, the jet model now also includes a synchrotron cut-off associated with the maximum energy of the electrons (see the discussion in Section 4).

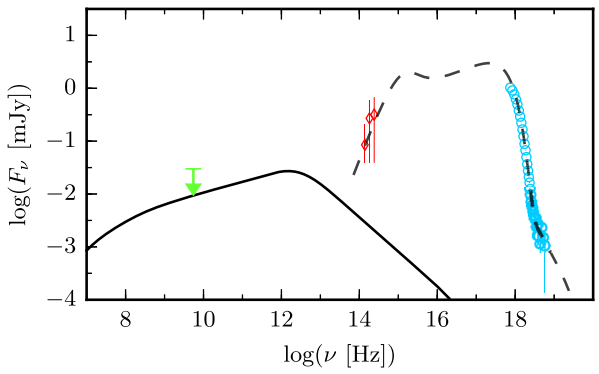

Figure 3. Broad-band spectra of H1743–322 in the soft state. The radio upper limit is plotted in green and the near-infrared and the X-ray observations are in red and blue, respectively. The vertical error bars represent the statistical and systematic errors on the mean. The total self-absorbed synchrotron jet emission from our model, averaged over the whole duration of the simulation, is shown as solid black. X-ray emission is used here solely as upper limits to define the feasibility of our fit. Its emission is fitted with the irradiated accretion disc DISKIR model, shown in dashed line.

In this case, the predicted jet synchrotron emission in X-rays is not much below the measured *RXTE* flux. As the internal shock model also predicts strong variability of the synchrotron emission (see Malzac 2014; D15), the jet may contribute significantly to the X-ray variability. If this was the case, the use of the X-ray PDS as a tracer of the accretion flow variability would be questionable and our implementation of the model would not be fully self-consistent. For this reason, in this work, we reduced the maximum energy of the electrons to a much lower value of $\gamma_{\rm max} = 5 \times 10^3$. As can be seen in the right-hand panel of Fig. 2, this change has negligible effects on the shape and normalization of the radio to IR SED, but implies the synchrotron emission is cut off below the energy range of *RXTE*. This ensures that the jet does not contribute at all to the observed fast hard X-ray variability used as model input. We note that the synchrotron cut-off is not taken into account in the current version of ISHEM. The exponential cut-off was simply added to the model a posteriori at an energy determined from $\gamma_{\rm max}$ and the average magnetic field in the optically thin region. There are no strong observational constraints on the location of the synchrotron cut-off in GX339–4, and we do not exclude that this cut-off could be located at higher energies. In this case, the contribution of modelled jet synchrotron to the *RXTE* band could be strongly reduced by choosing a steeper index for the electron energy distribution p. In the hard state of GX339–4, the 1σ uncertainties on the measurement of the optically thin spectral slope in infrared (Gandhi et al. 2011) would allow for p to be increased up to $p \simeq 3$. This would remain consistent with acceleration models and would dramatically reduce the jet contribution in X-rays, but other parameters of the model, such as the jet kinetic power or opening angle, would have to be changed in order to fit the hard state radio-IR SED. Finally, we

Table 1. Parameters of the DISKIR models shown in Figs 2 and 3, the inner irradiation fraction, $f_{\rm in}$, is fixed to 0.1 in all models. The Galactic absorption column $N_{\rm H}$ was fixed to 0.4 and 2×10^{22} cm^{-2} in GX339–4 and H1743–322, respectively.

	$kT_{\rm disc}$ (keV)	Γ	$kT_{\rm e}$ (keV)	$L_{\rm c}/L_{\rm d}$	$f_{\rm out}$	$R_{\rm irr}/R_{\rm in}$	$\log \frac{R_{\rm out}}{R_{\rm in}}$	Normalization
GX339–4 (hard)	0.19	1.61	44	4.6	0.04	2	3.8	10^5
GX339–4 (soft)	0.80	2.34	915	0.14	1.6×10^{-2}	1.01	4.8	2693
H1743–322 (soft)	0.98	2.22	200	0.014	7.92×10^{-4}	10	4.1	1120

note that the PDS of the optically thin jet synchrotron emission predicted by the model is not very different from the PDS of the input fluctuations (see Malzac 2014), so even if the jet dominates the X-ray variability, the observed X-ray PDS may remain a reasonable tracer of the fluctuations in the accretion flow.

5 DISCUSSION

Our results show that there is no need for a dramatic change in the jet properties in the soft state (such as a decrease of its total kinetic power). The drop in jet radiative efficiency due to the smaller amplitude of the fluctuations in the soft state quantitatively accounts for the quenching of the radio emission and is consistent with the current upper limits, although in the case of GX339–4, a minor change in the jet geometry is also required. The reader should note that the non-simultaneity of the X-ray PDS and the radio observations in the case of GX339–4 could also explain the slight overprediction of the model. Alternatively, an increase of the average jet Lorentz factor in the soft state could also reduce considerably the observed radio flux due to the beaming effects (Maccarone 2005). Of course, one cannot exclude that some other jet properties change at the hard to soft transition. In particular, a modest decrease of the jet power could also occur and would produce an even fainter radio emission, but we have performed the present analyses under the most conservative conditions.

The major point limiting the results is the interpretation of the X-ray PDS timing information in the soft state. In the hard state, the X-ray emission is dominated by the Comptonized emission from the hot flow/corona, which is strongly variable. Whereas in the soft state, a very stable disc component dominates over that of the corona and causes the observed X-ray PDS with weak variability. The variability of the weak non-thermal tail in the soft state is poorly known but observations of Cyg X-1 suggest that it is at least as variable as in the hard state (Churazov, Gilfanov & Revnivtsev 2001; Gierlinski, Zdziarski & Done 2010). The disc contribution to the X-ray PDS appears to overshadow that of a strongly varying corona. We found indications that this is the case in GX339–4 and H1743–322. The quality of the soft-state data sets considered in this paper is not good enough to disentangle accurately the disc and coronal components. But for both sources, we detect a significant increase of rms variability amplitude with energy band. For instance, in GX339–4, the 0.07–5 Hz rms amplitude variability increases from 1.49 per cent in the (disc-dominated) 2.5–5.7 keV band to 8.8 per cent in the (corona-dominated) 7–15 keV band. Unfortunately, the low count rate in the hard band prevents a good determination of the PDS that could be used as input to our model. However, it is obvious that the higher rms would lead to radio fluxes that are above the current observed limits for GX339–4.

In the framework of our model, this implies that the soft-state jet is driven by the disc rather than the corona. This is not unexpected. Indeed, there is reasonable evidence suggesting that the hard-state corona takes the form of a hot, optically thin, hard X-ray emitting accretion flow (see e.g. Done et al. 2007) that constitutes the central part of the accretion flow and probably drives the jet. In the soft state, this hot flow is replaced by a thermally emitting accretion disc extending down to the last stable orbit. Such disc may also launch a jet. The nature of the soft-state corona is not elucidated and is probably of very different nature from that of the hard state. It is perhaps unrelated to the jet. For instance, it was suggested that the soft-state corona could be made of small-scale active magnetic regions above and below the accretion disc (Zdziarski et al. 2002). The weak non-thermal hard X-ray emission of the soft state appears to have spectral and timing properties that are very different from that of the hot flow emission in hard state (Done et al. 2007). The jets launched from the strongly variable hot accretion flow of the hard state and the jets launched from the much steadier accretion disc of the soft state will have a very different appearance, even if both kind of jets have similar properties and kinetic power.

We note that the radio quenching may also be related to the change in variability pattern of the disc, which appears to be strongly variable in the hard state and very stable in the soft state (Uttley et al. 2011; De Marco et al. 2015). Alternatively, it is possible that the jet variability is associated only to the band limited X-ray noise observed in the hard state and not to the flicker noise component of the soft state. In either case, the predicted radio flux in the soft state would be much lower than what is obtained here using the full X-ray variability as input to the model. This would make the detection of soft state jets even more elusive. In any case, our results illustrate that the radio emission is not a robust tracer of the jet kinetic power, especially in the soft state.

Is the presence of dark jets in the soft state of X-ray binaries consistent with jet launching models? Hot and geometrically thick accretion flows are generally believed to be more efficient at launching jets than the thin discs of the soft state (Meier 2001; Sikora & Begelman 2013; Avara, McKinney & Reynolds 2016). However, recent studies of accretion disc coupled to a jet through the Blandford & Payne (1982) mechanism indicate that thin discs can eject a larger fraction of the accretion power than geometrically thick discs (Petrucci et al. 2010). In fact, from a theoretical point of view, the thermal disc-dominated state may harbour an even more powerful jet than the hard state.

Finally, we note that a weak jet was reported in the soft state of Cyg X-1 (Rushton et al. 2012). In this source, the radio flux is often detected in softer states. The radio emission is correlated with the coronal emission in all states, from soft to hard, which points to the jet activity being driven by the hot corona (Zdziarski et al. 2011). However, the soft states of Cyg X-1 are characterized by a much stronger coronal component and X-ray variability than those of the sources, like GX339–4 or H1743–322, where a strong radio

quenching is observed. In fact, Cyg X-1 does not seem to reach the canonical soft state. Besides, the jetted emission of Cyg X-1 is likely to be more complex than in classical transient low-mass X-ray binaries because of the interaction of the jet with the wind of its supergiant companion that may cause both additional jet dissipation and free–free absorption.

6 CONCLUSIONS

We have shown that in the context of the internal shock model, the suppression of the radio emission in soft state is naturally expected even if a jet is still present and as powerful as in the hard state. Although we do not rule out the jet quenching paradigm, the possible presence of a powerful dark jet in the soft state of X-ray binaries should be investigated further. The compared evolution of the radio spectrum and X-ray PDS during state transition could bring new constraints on the evolution of the jet properties between the hard and soft states. In addition, further investigations are needed to clarify the respective variability behaviour of the spectral components associated with the disc and corona in the different spectral state in order to determine which component drives the jet variability. Moreover, our predictions of radio emission are not far from the upper limits currently available. Our results for GX339–4 already indicate that some properties of the jets must change during the transition even if their power remains the same. Deeper radio observations and future *James Webb Space Telescope* mid-IR spectra can bring more constraints and help determine if indeed a dark jet is present in X-ray binary sources in the soft state. Finally, the search for evidence for the interaction of jets with their environment could be a way to detect dark jets in long-term soft sources.

ACKNOWLEDGEMENTS

The authors thank the anonymous referee for useful comments. JM thanks the Institute of Astronomy (Cambridge) for hospitality. SD thanks the Observatoire Midi-Pyrénées (Tarbes) for hospitality. This work is part of the CHAOS project ANR-12-BS05-0009 supported by the French Research National Agency (http://www.chaos-project.fr). PG acknowledges support from STFC (grant reference ST/J003697/2). This paper has made use of up-to-date SMARTS optical/near-infrared light curves that are available at www.astro.yale.edu/smarts/xrb/home.php. The Yale SMARTS XRB team is supported by NSF grants 0407063 and 070707 to Charles Bailyn. This research has made use of a collection of ISIS functions (ISISscripts) provided by ECAP/Remeis observatory and MIT (http://www.sternwarte.uni-erlangen.de/isis/).

REFERENCES

Avara M. J., McKinney J. C., Reynolds C. S., 2016, MNRAS, 462, 636
Belloni T. M., Stella L., 2014, Space Sci. Rev., 183, 43
Beloborodov A. M., 2000, ApJ, 539, L25
Blandford R. D., Payne D. G., 1982, MNRAS, 199, 883
Böttcher M., Dermer C. D., 2010, ApJ, 711, 445
Buxton M. M., Bailyn C. D., Capelo H. L., Chatterjee R., Dinçer T., Kalemci E., Tomsick J. A., 2012, AJ, 143, 130
Chaty S., Dubus G., Raichoor A., 2011, A&A, 529, A3
Chaty S., Muñoz Arjonilla A. J., Dubus G., 2015, A&A, 577, A101
Churazov E., Gilfanov M., Revnivtsev M., 2001, MNRAS, 321, 759
Clavel M., Rodriguez J., Corbel S., Coriat M., 2016, Astron. Nachr., 337, 435
Corbel S., Fender R. P., 2002, ApJ, 573, L35
Corbel S., Fender R. P., Tzioumis A. K., Nowak M., McIntyre V., Durouchoux P., Sood R., 2000, A&A, 359, 251
Coriat M., Corbel S., Buxton M. M., Bailyn C. D., Tomsick J. A., Körding E., Kalemci E., 2009, MNRAS, 400, 123
Daigne F., Mochkovitch R., 1998, MNRAS, 296, 275
De Marco B., Ponti G., Muñoz-Darias T., Nandra K., 2015, MNRAS, 454, 2360
Done C., Gierliński M., Kubota A., 2007, A&AR, 15, 1
Drappeau S., Malzac J., Belmont R., Gandhi P., Corbel S., 2015, MNRAS, 447, 3832
Fender R. P., 2001, MNRAS, 322, 31
Fender R., Gallo E., 2014, Space Sci. Rev., 183, 323
Fender R. P., Pooley G. G., Durouchoux P., Tilanus R. P. J., Brocksopp C., 2000, MNRAS, 312, 853
Fender R. P., Belloni T. M., Gallo E., 2004, MNRAS, 355, 1105
Fender R. P., Homan J., Belloni T. M., 2009, MNRAS, 396, 1370
Fuchs Y. et al., 2003, A&A, 409, L35
Gallo E., Fender R. P., Pooley G. G., 2003, MNRAS, 344, 60
Gallo E., Fender R., Kaiser C., Russell D., Morganti R., Oosterloo T., Heinz S., 2005, Nature, 436, 819
Gandhi P. et al., 2011, ApJ, 740, L13
Ghisellini G., Tavecchio F., Maraschi L., Celotti A., Sbarrato T., 2014, Nature, 515, 376
Gierliński M., Done C., Page K., 2008, MNRAS, 388, 753
Gierliński M., Done C., Page K., 2009, MNRAS, 392, 1106
Gierlinski M., Zdziarski A. A., Done C., 2010, preprint (arXiv:1011.5840)
Jamil O., Fender R. P., Kaiser C. R., 2010, MNRAS, 401, 394
Jourdain E., Roques J. P., Chauvin M., Clark D. J., 2012, ApJ, 761, 27
Jourdain E., Roques J. P., Malzac J., 2012, ApJ, 744, 64
Kaiser C. R., Sunyaev R., Spruit H. C., 2000, A&A, 356, 975
Körding E. G., Fender R. P., Migliari S., 2006, MNRAS, 369, 1451
Laurent P., Rodriguez J., Wilms J., Cadolle Bel M., Pottschmidt K., Grinberg V., 2011, Science, 332, 438
McClintock J. E., Remillard R. A., Rupen M. P., Torres M. A. P., Steeghs D., Levine A. M., Orosz J. A., 2009, ApJ, 698, 1398
McConnell M. L. et al., 2000, ApJ, 543, 928
Maccarone T. J., 2005, MNRAS, 360, L68
Malyshev D., Zdziarski A. A., Chernyakova M., 2013, MNRAS, 434, 2380
Malzac J., 2013, MNRAS, 429, L20
Malzac J., 2014, MNRAS, 443, 299
Malzac J., 2016, Astron. Nachr., 337, 391
Meier D. L., 2001, in Wheeler J. C., Martel H., eds, AIP Conf. Ser. Vol. 586, Relativistic Astrophysics. Am. Inst. Phys., New York, p. 420
Petrucci P. O., Ferreira J., Henri G., Malzac J., Foellmi C., 2010, A&A, 522, A38
Rees M. J., 1978, MNRAS, 184, 61P
Rees M. J., Meszaros P., 1994, ApJ, 430, L93
Rodriguez J., Varnière P., 2011, ApJ, 735, 79
Rodriguez J. et al., 2015, ApJ, 807, 17
Rushton A. et al., 2012, MNRAS, 419, 3194
Russell D. M., Miller-Jones J. C. A., Maccarone T. J., Yang Y. J., Fender R. P., Lewis F., 2011, ApJ, 739, L19
Sault R. J., Teuben P. J., Wright M. C. H., 1995, in Shaw R. A., Payne H. E., Hayes J. J. E., eds, ASP Conf. Ser. Vol. 77, Astronomical Data Analysis Software and Systems IV. Astron. Soc. Pac., San Francisco, p. 433
Shidatsu M. et al., 2011, PASJ, 63, 785
Sikora M., Begelman M. C., 2013, ApJ, 764, L24
Spada M., Ghisellini G., Lazzati D., Celotti A., 2001, MNRAS, 325, 1559
Steiner J. F., McClintock J. E., Reid M. J., 2012, ApJ, 745, L7
Stirling A. M., Spencer R. E., de la Force C. J., Garrett M. A., Fender R. P., Ogley R. N., 2001, MNRAS, 327, 1273
Uttley P., Wilkinson T., Cassatella P., Wilms J., Pottschmidt K., Hanke M., Böck M., 2011, MNRAS, 414, L60

Zanin R., Fernández-Barral A., de Oña-Wilhelmi E., Aharonian F., Blanch O., Bosch-Ramon V., Galindo D., 2016, A&A, 596, A55
Zdziarski A. A., Poutanen J., Paciesas W. S., Wen L., 2002, ApJ, 578, 357
Zdziarski A. A., Gierliński M., Mikołajewska J., Wardziński G., Smith D. M., Harmon B. A., Kitamoto S., 2004, MNRAS, 351, 791
Zdziarski A. A., Skinner G. K., Pooley G. G., Lubiński P., 2011, MNRAS, 416, 1324
Zdziarski A. A., Lubiński P., Sikora M., 2012, MNRAS, 423, 663
Zdziarski A. A., Pjanka P., Sikora M., Stawarz Ł., 2014, MNRAS, 442, 3243
Zdziarski A. A., Malyshev D., Chernyakova M., Pooley G. G., 2016, preprint (arXiv:e-prints)

This paper has been typeset from a TEX/LATEX file prepared by the author.